

Enhancing violations of single-site Leggett-Garg inequalities in nonequilibrium correlated many-body systems by interactions and decoherence

J. J. Mendoza-Arenas,^{1,*} F. J. Gómez-Ruiz,¹ F. J. Rodríguez,¹ and L. Quiroga¹

¹*Departamento de Física, Universidad de los Andes, A.A. 4976, Bogotá D. C., Colombia*

We discuss the existence of genuine quantum transport in open many-body systems through the violation of Leggett-Garg inequalities. Considering a testbed nonequilibrium configuration, we show that particle interactions control the direction and amplitude of maximal violation, and that in the strongly-interacting and strongly-driven regime bulk dephasing enhances the violation. Through an analytical study of a minimal model we unravel the basic ingredients to explain this decoherence-enhanced quantumness, illustrating that such an effect emerges in a wide variety of systems.

Introduction.— For several decades, assessing the existence of genuine quantum behavior [1] and quantifying coherence in quantum systems [2] have remained as fundamental open problems, critical to applications in computation and information processing. A seminal breakthrough in this direction was made by Leggett and Garg [3, 4], who considered the conditions that a macroscopic system entirely described by classical physics should satisfy. These are macroscopic realism (a system’s property is well defined at every time regardless of whether it is observed or not) and noninvasive measurability (the system is unaffected by measurements on it). When these conditions are met, the system satisfies the so-called Leggett-Garg inequalities (LGIs). The experimental observation of their violation, which serves as witness of quantum coherence, has been sought intensively and reported in various platforms [5–9].

In order to establish realistic conditions where LGIs are maximally violated, providing optimal settings for quantum protocols performed in a particular system, its unavoidable coupling to the environment has to be considered. Recent theoretical research on few-qubit systems has determined that Markovian noise degrades quantumness [10–14], while non-Markovianity helps restore it [15–17]. However, many-body interacting systems, where spectacular effects resulting from quantum coherence emerge, remain unexplored within this effort. The non-trivial impact of dissipation in multilevel systems is known to induce unexpected beneficial effects, as entanglement generation and quantum state engineering [18–21], restoration of hidden quantum phase transitions [22] and environment-assisted transport [23–26]. Thus such systems constitute attractive candidates for uncovering novel mechanisms of LGI violation enhancement.

In the present work we establish such mechanisms in testbed open many-body systems. We show that not only particle interactions, but also bulk dephasing, can increase the violation of LGIs in Markovian systems. For this we assess the quantumness of the transport supported by interacting spin chains when driven out of equilibrium by unequal boundary reservoirs, a configuration considered so far for LGIs on single-particle systems only [27, 28]. Using a minimal model to illustrate

the basic ingredients responsible for this phenomenon, we argue that it can emerge under a wide range of conditions, being a powerful strategy for strengthening the quantumness of a system.

Nonequilibrium setup.— We consider a spin-1/2 chain coupled to two reservoirs of unequal magnetization at its boundaries, as depicted in Fig. 1. These induce a net homogeneous spin current in its nonequilibrium steady state (NESS) [29–33]. The chain is characterized by the one-dimensional XXZ Hamiltonian

$$\hat{\mathcal{H}} = \tau \sum_{n=1}^{L-1} [\hat{\sigma}_n^x \hat{\sigma}_{n+1}^x + \hat{\sigma}_n^y \hat{\sigma}_{n+1}^y + \Delta \hat{\sigma}_n^z \hat{\sigma}_{n+1}^z], \quad (1)$$

where $\hat{\sigma}_n^\alpha$ are the Pauli matrices ($\alpha = x, y, z$), L is the number of sites, τ is the exchange interaction (we set the energy scale by taking $\tau = 1$), and Δ is the anisotropy along z direction; we take $\Delta \geq 0$ without loss of generality. When mapping the model to a spinless-fermion description, τ corresponds to the hopping and $\tau\Delta$ to a density-density interaction; thus $\Delta > 1$ is referred to as the strongly-interacting regime.

The dynamics of the chain under the influence of the environment is modeled by a Lindblad master equation [34],

$$\dot{\hat{\rho}}_t = \hat{\mathcal{L}}(\hat{\rho}) = -i[\hat{\mathcal{H}}, \hat{\rho}] + \sum_k \hat{V}_k \hat{\rho} \hat{V}_k^\dagger - \frac{1}{2} \{ \hat{V}_k^\dagger \hat{V}_k, \hat{\rho} \}. \quad (2)$$

Here $\hat{\rho}$ is the density matrix of the chain, $\hat{\mathcal{L}}$ is the Lindblad superoperator, $\{.,.\}$ is the anticommutator of two operators, and \hat{V}_k correspond to the jump operators establishing the coupling of the chain to the environment. For the boundary driving we consider operators that annihilate (\hat{V}^-) and create (\hat{V}^+) spin excitations at both the left (ℓ) and right (r) edges of the chain, given by $\hat{V}_{r,\ell}^- = \sqrt{\Gamma(1 \mp f)} \hat{\sigma}_{1,L}^-$ and $\hat{V}_{r,\ell}^+ = \sqrt{\Gamma(1 \pm f)} \hat{\sigma}_{1,L}^+$.

Here Γ is the coupling strength (we take $\Gamma = 1$) and the driving $0 \leq f \leq 1$ establishes the magnetization imbalance between the boundaries. If $f = 0$, spin excitations are created and annihilated at the same rate on both boundaries, so there is no net magnetization imbalance and thus no spin transport. If $f > 0$, more excitations are

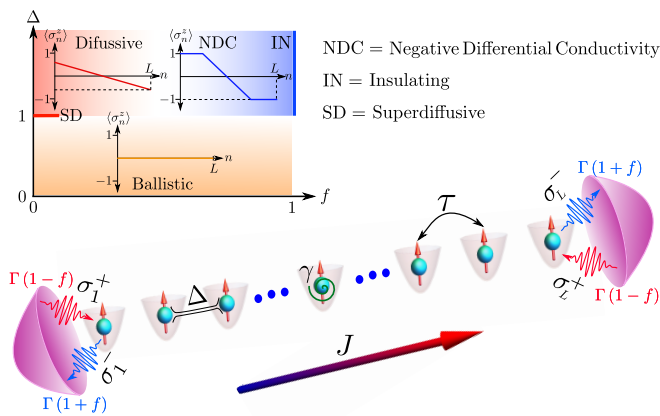


FIG. 1. **Scheme of the system under study.** An XXZ spin chain is coupled to unequal reservoirs at its boundaries, which drive it to a NESS where a spin current J flows from left to right. The nonequilibrium Δ - f phase diagram is also shown, where characteristic magnetization profiles are depicted for each conduction regime. These correspond to a flat profile for ballistic transport, a ramp with homogeneous slope for diffusion, and ferromagnetic domains for the insulating state.

created (annihilated) on the left-most (right-most) site of the lattice, inducing a net current resulting from a left-to-right flow and its weaker backflow. We also consider bulk dephasing processes, modeled by jump operators $\hat{V}_n^z = \sqrt{\gamma} \hat{\sigma}_n^z$ ($n = 1, \dots, L$), where γ is the homogeneous dephasing rate. These operators can be obtained following standard microscopic derivations of Lindblad equations. The driving results after tracing out the degrees of freedom of both reservoirs, and the dephasing from the coupling of the chain to local vibrational degrees of freedom [30, 34].

When the spin chain evolves in time as dictated by Eq. (2), it eventually reaches its unique NESS, given by $\hat{\rho}_\infty = \lim_{t \rightarrow \infty} \hat{\rho}(t) = \lim_{t \rightarrow \infty} \exp[\hat{\mathcal{L}}(t)] \hat{\rho}(0)$, with $\hat{\rho}(0)$ an initial state. Its transport properties are characterized by its magnetization profile $\langle \hat{\sigma}_n^z \rangle$ and the homogeneous spin current $J = \langle \hat{J}_n \rangle$, with $\hat{J}_n = 2(\hat{\sigma}_n^x \hat{\sigma}_{n+1}^y - \hat{\sigma}_n^y \hat{\sigma}_{n+1}^x)$. The phase diagram of the dephasing-free model, obtained from the behavior of both quantities, is depicted in Fig. 1. For weak driving f (linear response), $\Delta < 1$ shows ballistic conduction while for $\Delta > 1$ the system satisfies a normal diffusion equation [29, 30]. This indicates a nonequilibrium quantum phase transition at the isotropic point $\Delta = 1$, which is super-diffusive [35]. For large driving f and $\Delta > 1$, negative differential conductivity (NDC) emerges, leading to an insulating state at maximal driving $f = 1$ in which opposite-polarized ferromagnetic domains suppress transport [30, 31]. This behavior is absent at $\Delta < 1$, where transport remains ballistic for any f .

In the presence of dephasing, spin transport is monotonically degraded with γ and becomes diffusive for $\Delta <$

1 [36], while it is largely enhanced with γ for $\Delta > 1$, a manifestation of strong correlations [31]. The enhancement vastly increases with driving, as dephasing washes out the NDC and induces an insulator-conducting transition at $f = 1$.

LGI's calculation.— As shown by Leggett and Garg [3, 4], macroscopic classical systems satisfy the inequality $\mathcal{C}(t_1, t_2) + \mathcal{C}(t_2, t_3) - \mathcal{C}(t_1, t_3) \leq 1$ ($t_1 < t_2 < t_3$). Here $\mathcal{C}(t_i, t_j)$ denotes the two-time correlations of a dichotomic operator \hat{Q} (with eigenvalues ± 1) between times t_i and t_j , and is given by $\mathcal{C}(t_i, t_j) = \frac{1}{2} \langle \{ \hat{Q}(t_i), \hat{Q}(t_j) \} \rangle$. For the NESS $\hat{\rho}_\infty$, which is unaffected by an evolution under $\hat{\mathcal{L}}$, this correlation with $t_i < t_j$ is given by

$$\mathcal{C}(t_i, t_j) = \text{Re} \left(\text{Tr} \left[\hat{Q} \exp \left[\hat{\mathcal{L}}(t_j - t_i) \right] \hat{Q} \hat{\rho}_\infty \right] \right). \quad (3)$$

Thus, $\mathcal{C}(t_i, t_j) = \mathcal{C}(0, t_j - t_i)$, and taking time intervals $t_2 - t_1 = t_3 - t_2 = t$, the LGI reduces to $\mathcal{K}(t) \equiv 2\mathcal{C}(t) - \mathcal{C}(2t) \leq 1$, where we define the Leggett-Garg function $\mathcal{K}(t)$, and $\mathcal{C}(t) \equiv \mathcal{C}(0, t)$. We assess genuine quantum behavior when this inequality is violated.

We focus on LGIs when performing measurements of local observables $\hat{Q} = \hat{\sigma}_l^\alpha$ ($\alpha = x, z$) for site $l = L/2$ on the NESS $\hat{\rho}_\infty$. To evaluate their violation in the boundary-driven setup for large systems, we obtain their NESS applying the time-dependent density matrix renormalization group [37, 38], describing the state by a matrix product structure [29, 39]. Then we calculate the time evolution of Eq. (3) to obtain the single-site two-time correlations, from which the Leggett-Garg function $\mathcal{K}(t)$ follows immediately. Our simulations are based on the open-source Tensor Network Theory (TNT) library [40, 41]. This constitutes a novel and topical application of matrix product states, fueled by the growing interest in evaluating two-time correlations in dissipative many-body systems [42–46].

Controlling LGI violations with interactions: dephasing free case.— We now show that violations of LGIs can be tuned by interactions, and can indicate nonequilibrium quantum phase transitions. For this we consider the linear-response regime, where the system presents a transition from ballistic ($\Delta < 1$) to diffusive ($\Delta > 1$) spin transport. In the upper panels of Fig. 2 we show $\mathcal{C}_\alpha(t)$ for $\alpha = x, z$, which measure the response of the system when adding or removing a spin excitation for $\alpha = x$, or measuring the local magnetization for $\alpha = z$. These correlations already show a qualitative difference, most notable for early times, between the two transport regimes. First, since for $\Delta = 0$ and weak driving the NESS is very close to an identity [47, 48] (with terms of $\mathcal{O}(f)$ accounting for the spin current and magnetization and higher-order corrections for correlations), the results are very well approximated by known analytical results for infinite-temperature state. These correspond to an

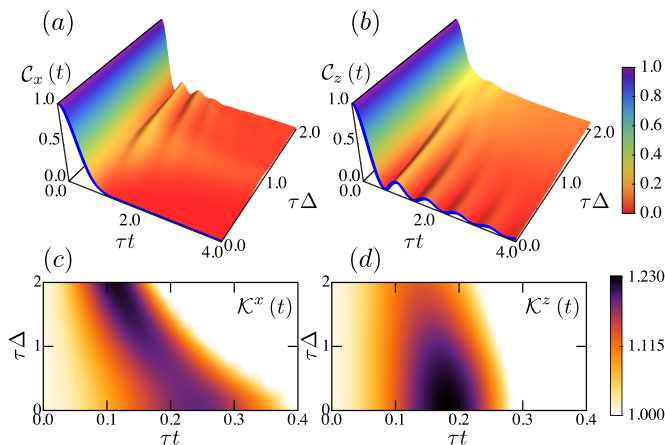


FIG. 2. Time correlations $C_\alpha(t)$ (upper panels) and Leggett-Garg functions $\mathcal{K}^\alpha(t)$ (lower panels) as a function of time and anisotropy Δ for weak driving $f = 0.1$ and system size $L = 60$. (a), (c): $\alpha = x$. (b), (d): $\alpha = z$. In the lower panels, LGI violations occur for the colored regions, while classical transport corresponds to the white regions. The blue lines in the upper panels are the infinite-temperature results described in the main text for $\Delta = 0$.

exponential decay [49] for $\alpha = x$, $C_x(t) \approx e^{-4\tau^2 t^2}$, and a squared Bessel function [50] for $\alpha = z$, $C_z(t) \approx \mathcal{J}_0^2(4\tau t)$, thus being independent of the details of the driving. The qualitative behavior continues when increasing Δ approximately till the isotropic point. For the strongly interacting regime, the correlations $C_x(t)$ develop early oscillations of frequency $\sim \Delta^{-1}$, while those of $C_z(t)$ are strongly suppressed.

In the lower panels of Fig. 2 we show the corresponding Leggett-Garg functions; these are obtained exactly for $\Delta = 0$, namely $\mathcal{K}^x(t) = 2e^{-4\tau^2 t^2} - e^{-16\tau^2 t^2}$ and $\mathcal{K}^z(t) = 2\mathcal{J}_0^2(4\tau t) - \mathcal{J}_0^2(8\tau t)$, which agree with our numerical simulations. For all Δ and early times the inequalities in both directions are violated, indicating genuine quantum behavior which cannot be reproduced by classical physics¹. In Fig. 3 we show the maximal violations $\mathcal{K}_{\text{Max}}^\alpha$ as a function of Δ , and observe that while the function of $\alpha = z$ monotonically decreases with interactions, that of $\alpha = x$ has a non-monotonic behavior, but increases for $\Delta > 1$. Moreover, at the isotropic point the direction along which the LGI violation becomes maximal changes, from $\alpha = z$ for $\Delta < 1$ to $\alpha = x$ for $\Delta > 1$. As a result, the direction and magnitude of the overall maximal violation can be controlled by Δ , so that in the strongly-interacting regime the quantum behavior is enhanced by interactions. This also shows that the LGI

¹ We do not consider longer times, where revivals of the quantum behavior occur, as we are mostly interested in the maximal violations $\mathcal{K}_{\text{Max}}^\alpha$, which take place at an early time.

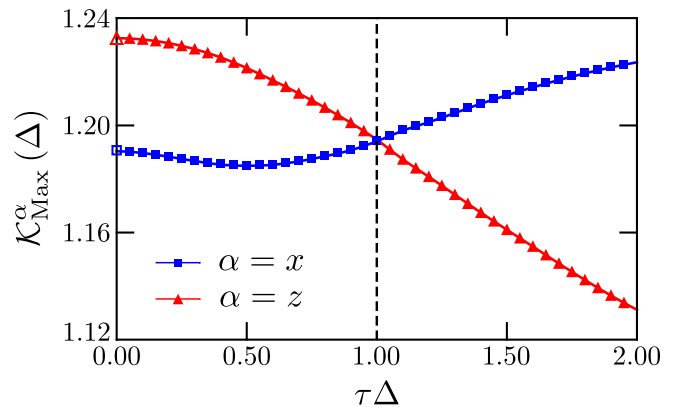


FIG. 3. Maximum violation of LGI along x and z directions as a function of anisotropy Δ , for weak driving $f = 0.1$ and size $L = 60$. The open symbols at $\Delta = 0$ correspond to the infinite-temperature results as described in the main text.

violation indicates the nonequilibrium critical point, a property that it also features in equilibrium [51, 52].

Dephasing-enhanced LGI violations.— Now we discuss LGIs of the driven system in the presence of bulk dephasing. As previously mentioned, for strong interactions $\Delta > 1$ and large driving $f = 1$ dephasing melts the ferromagnetic domains that suppress transport, inducing a transition to a conducting state. Thus the spin current is enhanced with γ by several orders of magnitude, as shown in the main panel of Fig. 4. This constitutes a many-body scheme of environment-assisted transport [31]. Here we calculate the maximum violation of the LGI for $\alpha = z$ as a function of γ , also shown in the main panel of Fig. 4. Small systems are considered to be able to calculate the NESS in the absence of (or for very weak) dephasing, which takes an exponentially-long time due to the presence of the ferromagnetic domains [30, 31].

For $\gamma = 0$ LGIs are violated, since operator \hat{Q} is applied between the ferromagnetic domains and induces appreciable dynamics. But remarkably, as the system becomes conducting due to weak dephasing, it also presents enhanced quantumness manifested in the increase of the violations. Even for stronger dephasing $\gamma \approx 1$, where $\mathcal{K}_{\text{Max}}^z$ decreases with γ , the violation is still larger than that of $\gamma = 0$. Thus there is a wide range of environmental couplings where in addition to a large transport enhancement, quantum features are strengthened. This is in stark contrast to the weakly-interacting case, depicted in Fig. 1 of the Supplemental Material (SM) [53], where not only the spin transport is monotonically degraded with dephasing, but also the violation of LGIs and thus the quantumness of the NESS. This indicates that the origin of the observed effect is truly a consequence of strong interactions between particles, a situation where the behavior of LGIs is still largely unexplored.

We also observe enhanced violation of LGIs with de-

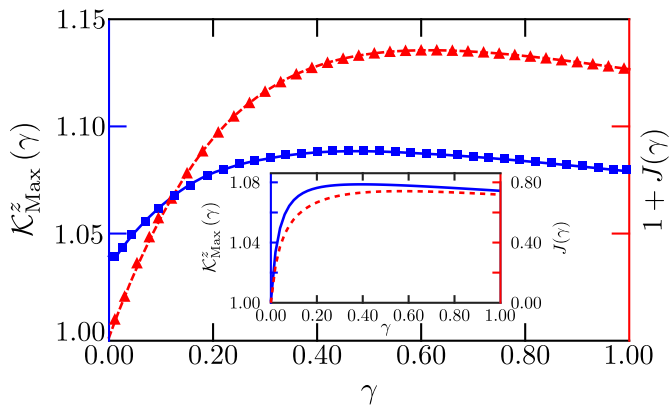


FIG. 4. Maximum violation of LGI for the XXZ chain along z direction (blue solid line, squares) and shifted spin current (red dashed line, triangles) as a function of dephasing γ , for system size $L = 16$, anisotropy $\Delta = 2$ and maximal driving $f = 1$. Inset: Maximal violation (blue solid line) and current (red dashed line) for the minimal model with $f = 1$, $K = 10$, $\delta = 1$ and $\Gamma = 1$.

phasing even for much weaker driving f , where for $\gamma = 0$ the system is conducting and the differential conductivity is positive [30, 31] (see SM). These results show that not only inducing a backflow in the lattice, but also (and more surprisingly) dephasing can enhance quantumness even when the system is not initially insulating. Furthermore, we also find an increase of violations with system size, which indicates that this is not a small-lattice effect. The latter strongly contrasts with the natural expectation that in conducting regimes, environmental coupling degrades LGI violations [27, 54].

Minimal model.— To obtain more insight into the incoherent enhancement of LGI violations, we analyze a simple model which incorporates the essential ingredients of the strongly-interacting lattice [31]. This model mimics its gapped eigenstructure, consisting of flat (insulating) and wide (conducting) bands, and the population transfer between them due to coherent processes, incoherent driving and dephasing. It consists of K levels $|1\rangle, \dots, |K\rangle$, with Hamiltonian

$$\hat{\mathcal{H}}_{\text{min}} = \frac{1}{2} \sum_{k=1}^{K-1} (|k\rangle\langle k+1| + \text{H.c.}) + \delta|K\rangle\langle K|, \quad (4)$$

where state $|K\rangle$ is elevated in energy with respect to the others by an amount $\delta > 0$; thus the bands are separated by a gap of $\mathcal{O}(\delta)$, similarly to the strongly-interacting XXZ model (gaps of $\mathcal{O}(\Delta)$). The driving is modeled by the incoherent coupling of states $|1\rangle$ and $|K\rangle$ to an auxiliary site. This leads to the emergence of NCD, an insulating state at $f = 1$ and dephasing-enhanced transport, as described in the SM [53]. To study LGIs, we calculate the time correlations for the operator $\hat{Q} = \hat{\mathcal{I}} - 2|P\rangle\langle P|$, where site P is taken away from the boundaries. Exact

numerical results of the Leggett-Garg function $\mathcal{K}(t)$ are depicted in the SM, showing that, similarly to the original model, two mechanisms enhance the violations of LGIs with respect to the dephasing-free $f = 1$ limit, namely introducing a backflow ($f < 1$) or dephasing ($\gamma > 0$). Thus in spite of its simplicity, the model features the essential ingredients underlying such phenomena.

Analytical results up to $\mathcal{O}((\delta)^{-2})$ for the strongly-driven limit, where the effects of decoherence are the largest, help determine how LGI violations are increased; see details in the SM [53]. For the dephasing-free system with $f = 1$, $\mathcal{C}^{(0)}(t) \approx \mathcal{K}^{(0)}(t) \approx 1$, so the LGI is not significantly violated, as expected. Defining $\beta = 2(1-f)(1+\Gamma^2)$ when slightly moving from maximal driving with $\gamma = 0$, or $\beta = 16\gamma(1+\Gamma^2)/\Gamma$ when introducing weak dephasing at $f = 1$, or their sum if both are present, we get the general behavior

$$\mathcal{K}(t) = 1 + \beta \left(\frac{t}{2\delta} \right)^2. \quad (5)$$

This shows that both mechanisms induce a violation of the LGI which grows quadratically at early times, and which increases linearly as $(1-f)$ and/or γ . It also manifests that the source of these results, also present in the strongly-interacting XXZ model, is the gapped eigenstructure of the model.

Conclusions.— We have assessed the quantumness of spin transport in a nonequilibrium many-body system coupled to different environments, analyzing Leggett-Garg inequalities. Using matrix product state simulations, we have determined that in the strongly-interacting regime, interactions and (unexpectedly) bulk dephasing can enhance their violation. The main mechanism behind the latter effect is illustrated by the same observation in a minimal model, which mimics the gapped eigenstructure of the original spin system. Given the simplicity of the studied models, our results pave the way for novel experimental protocols of detecting macroscopic quantum coherence in a large variety of scenarios, including single-particle and many-body inhomogeneous (e.g. disordered [32, 33]) current-carrying systems.

J.J.M.-A. thanks Stephen Clark and Katarzyna Roszak for interesting discussions. We acknowledge financial support from Vice-Rectoría de Investigaciones through UniAndes-2019 projects *Excited State Quantum Phase Transition in a Driven Dicke Model* and *Quantum thermalization and optimal control in many-body systems*. We acknowledge financial support from Departamento Administrativo de Ciencia, Tecnología e Innovación Colciencias, through the project *Producción y Caracterización de Nuevos Materiales Cuánticos de Baja Dimensionalidad: Criticalidad Cuántica y Transiciones de Fase Electrónicas*, CD 63414.

-
- [1] G. de Chiara and A. Sanpera, *Rep. Prog. Phys.* **81**, 074002 (2018).
- [2] A. Streltsov, G. Adesso, and M. B. Plenio, *Rev. Mod. Phys.* **89**, 041003 (2017).
- [3] A. J. Leggett and A. Garg, *Phys. Rev. Lett.* **54**, 857 (1985).
- [4] C. Emary, N. Lambert, and F. Nori, *Reports on Progress in Physics* **77**, 016001 (2014).
- [5] A. Palacios-Laloy, F. Mallet, F. Nguyen, P. Bertet, D. Vion, D. Esteve, and A. N. Korotkov, *Nat Phys* **6**, 442 (2010).
- [6] M. E. Goggin, M. P. Almeida, M. Barbieri, B. P. Lanyon, J. L. O'Brien, A. G. White, and G. J. Pryde, *Proceedings of the National Academy of Sciences* **108**, 1256 (2011).
- [7] G. C. Knee, S. Simmons, E. M. Gauger, J. J. Morton, H. Riemann, N. V. Abrosimov, P. Becker, H.-J. Pohl, K. M. Itoh, M. L. Thewalt, G. A. D. Briggs, and S. C. Benjamin, *Nat Comm* **3**, 606 (2012).
- [8] J. Dressel, C. J. Broadbent, J. C. Howell, and A. N. Jordan, *Phys. Rev. Lett.* **106**, 040402 (2011).
- [9] Z.-Q. Zhou, S. F. Huelga, C.-F. Li, and G.-C. Guo, *Phys. Rev. Lett.* **115**, 113002 (2015).
- [10] C. Emary, *Phys. Rev. A* **87**, 032106 (2013).
- [11] M. Lobejko, J. Luczka, and J. Dajka, *Phys. Rev. A* **91**, 042113 (2015).
- [12] A. Friedenberger and E. Lutz, *Phys. Rev. A* **95**, 022101 (2017).
- [13] T. Chanda, T. Das, S. Mal, A. Sen(De), and U. Sen, *Phys. Rev. A* **98**, 022138 (2018).
- [14] M. Ban, *Quantum Information Processing* **17**, 317 (2018).
- [15] P.-W. Chen and M. Ali, *Sci. Rep.* **4**, 6165 (2014).
- [16] J. Naikoo, S. Banerjee, and R. Srikanth, arXiv:1806.00537 (2018).
- [17] S. Datta, S. Mal, and A. Majumdar, arXiv:1808.10345 (2018).
- [18] S. Diehl, A. Micheli, A. Kantian, B. Kraus, H. P. Büchler, and P. Zoller, *Nat. Phys.* **4**, 878 (2008).
- [19] F. Verstraete, M. M. Wolf, and J. I. Cirac, *Nat. Phys.* **5**, 633 (2009).
- [20] Y. Lin, J. P. Gaebler, F. Reiter, T. R. Tan, R. Bowler, A. S. Sørensen, D. Leibfried, and D. J. Wineland, *Nature* **504**, 415 (2013).
- [21] D. Kienzler, H.-Y. Lo, B. Keitch, L. de Clercq, F. Leupold, F. Lindenefelder, M. Marinelli, V. Negnevitsky, and J. P. Home, *Science* **347**, 53 (2015).
- [22] G. Zhang, E. Novais, and H. U. Baranger, *Phys. Rev. Lett.* **118**, 050402 (2017).
- [23] M. B. Plenio and S. F. Huelga, *New J. Phys.* **10**, 113019 (2008).
- [24] M. Mohseni, P. Rebentrost, S. Lloyd, and A. Aspuru-Guzik, *J. Chem. Phys.* **129**, 174106 (2008).
- [25] A. W. Chin, A. Datta, F. Caruso, S. F. Huelga, and M. B. Plenio, *New J. Phys.* **12**, 065002 (2010).
- [26] I. Sinayskiy, A. Marais, F. Petruccione, and A. Ekert, *Phys. Rev. Lett.* **108**, 020602 (2012).
- [27] N. Lambert, C. Emary, Y.-N. Chen, and F. Nori, *Phys. Rev. Lett.* **105**, 176801 (2010).
- [28] J. C. Castillo, F. J. Rodríguez, and L. Quiroga, *Phys. Rev. A* **88**, 022104 (2013).
- [29] T. Prosen and M. Žnidarič, *J. Stat. Mech.* , P02035 (2009).
- [30] G. Benenti, G. Casati, T. Prosen, D. Rossini, and M. Žnidarič, *Phys. Rev. B* **80**, 35110 (2009).
- [31] J. J. Mendoza-Arenas, T. Grujic, D. Jaksch, and S. R. Clark, *Phys. Rev. B* **87**, 235130 (2013).
- [32] M. Žnidarič, A. Scardicchio, and V. Varma, *Phys. Rev. Lett.* **117**, 040601 (2016).
- [33] M. Žnidarič, J. J. Mendoza-Arenas, S. R. Clark, and J. Goold, *Annalen der Physik* **529**, 1600298 (2017).
- [34] H.-P. Breuer and F. Petruccione, *The theory of open quantum systems* (Oxford University Press, Oxford, 2002).
- [35] M. Žnidarič, *Phys. Rev. Lett.* **106**, 220601 (2011).
- [36] M. Žnidarič, *New Journal of Physics* **12**, 043001 (2010).
- [37] M. Zwolak and G. Vidal, *Phys. Rev. Lett.* **93**, 207205 (2004).
- [38] F. Verstraete, J. J. Garcia-Ripoll, and J. I. Cirac, *Phys. Rev. Lett.* **93**, 207204 (2004).
- [39] U. Schollwöck, *Annals of Physics* **326**, 96 (2011).
- [40] S. Al-Assam, S. R. Clark, D. Jaksch, and T. Development Team, “Tensor Network Theory Library, Beta Version 1.2.0,” (2016).
- [41] S. Al-Assam, S. R. Clark, and D. Jaksch, *J. Stat. Mech.* **2017**, 093102 (2017).
- [42] B. Sciola, D. Poletti, and C. Kollath, *Phys. Rev. Lett.* **114**, 170401 (2015).
- [43] B. Everest, I. Lesanovsky, J. P. Garrahan, and E. Levi, *Phys. Rev. B* **95**, 024310 (2017).
- [44] L. He, L. M. Sieberer, and S. Diehl, *Phys. Rev. Lett.* **118**, 085301 (2017).
- [45] R. R. W. Wang, B. Xing, G. G. Carlo, and D. Poletti, *Phys. Rev. E* **97**, 020202 (2018).
- [46] S. Wolff, J.-S. Bernier, D. Poletti, A. Sheikhan, and C. Kollath, arXiv:1809.10464 (2018).
- [47] M. Žnidarič, *J. Stat. Mech. Theor. Exp.* **2010**, L05002 (2010).
- [48] M. Žnidarič, *Phys. Rev. E* **83**, 011108 (2011).
- [49] H. W. Capel and J. H. H. Perk, *Physica A* **87A**, 211 (1977).
- [50] S. Katsura, T. Horiguchi, and M. Suzuki, *Physica* **46**, 67 (1970).
- [51] F. J. Gómez-Ruiz, J. J. Mendoza-Arenas, F. J. Rodríguez, C. Tejedor, and L. Quiroga, *Phys. Rev. B* **93**, 035441 (2016).
- [52] F. J. Gómez-Ruiz, J. J. Mendoza-Arenas, F. J. Rodríguez, C. Tejedor, and L. Quiroga, *Phys. Rev. B* **97**, 235134 (2018).
- [53] See the Supplemental Material at url will be inserted by publisher, for details of the calculations and derivations.
- [54] C. Robens, W. Alt, D. Meschede, C. Emary, and A. Alberti, *Phys. Rev. X* **5**, 011003 (2015)

—Supplemental Material—
Enhancing violations of single-site Leggett-Garg inequalities in nonequilibrium correlated many-body systems by interactions and decoherence

J. J. Mendoza-Arenas,¹ F. J. Gómez-Ruiz,¹ F. J. Rodríguez,¹ and L. Quiroga¹

¹*Departamento de Física, Universidad de los Andes, A.A. 4976, Bogotá D. C., Colombia.*

Contents

S1. Weakly-interacting system	1
S2. LGI violations in the minimal model	2
S3. Analytic results on the minimal model	2
A. Perturbative $1 - f$ solution to the minimal model	3
B. LGIs violation enhancement by driving	5
C. LGIs violation enhancement by dephasing	6
References	6

S1. WEAKLY-INTERACTING SYSTEM

In this section we briefly illustrate the impact of bulk dephasing on LGIs in the weakly-interacting regime ($\Delta < 1$) of the nonequilibrium model. In Fig. S1 we show how, similarly to spin transport, the violation of the inequalities for $\alpha = z$ is monotonically degraded with the dephasing rate γ . Thus the quantumness of the transport supported by the system is degraded by environmental coupling, as intuitively expected [S1]. It is worth noting that even for the largest values of dephasing considered, the inequalities are still violated, so the transport is still of quantum nature and its properties cannot be accounted for classically.

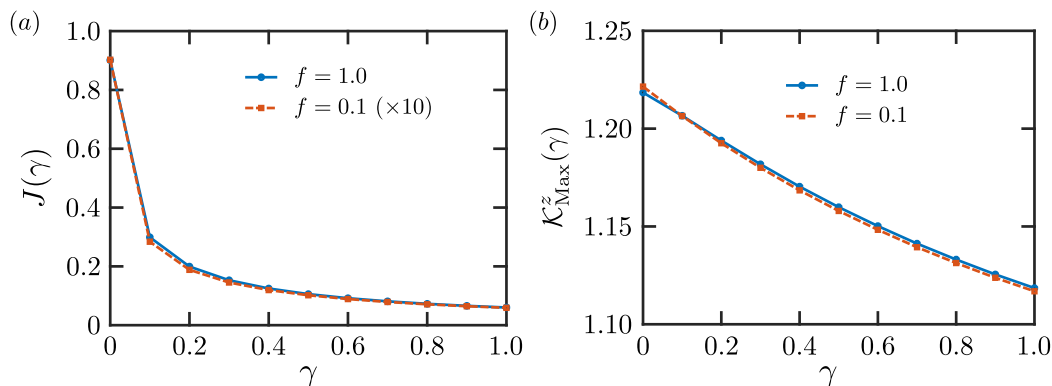


FIG. S1. **Weakly-interacting XXZ model.** (a) Spin current as a function of dephasing, for $L = 60$ sites, $\Delta = 0.5$, $\alpha = z$ and both weak ($f = 0.1$) and strong ($f = 1.0$) driving. (b) Corresponding maximal value of Leggett-Garg functions.

S2. LGI VIOLATIONS IN THE MINIMAL MODEL

Here we provide the details of the minimal model. A scheme is depicted in Fig. S2. The non-interacting lattice, with Hamiltonian given by Eq. (1) of the main text, has an associated local current operator given by

$$\hat{J}_{\text{min},k} = -i(|k\rangle\langle k+1| - \text{H.c.}). \quad (\text{S1})$$

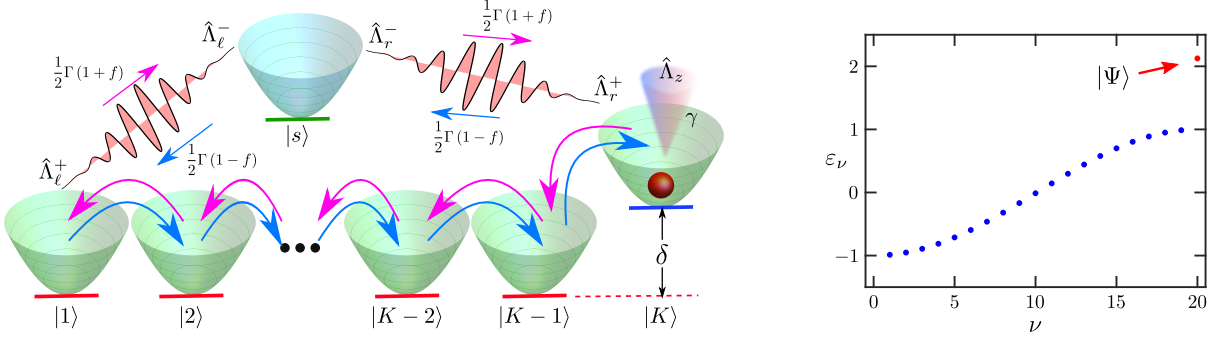


FIG. S2. **Minimal model.** (a) Schematic illustration. A single-particle system is incoherently coupled to an auxiliary state $|s\rangle$, which induces a current with driving f . (b) Eigenstructure. The depicted energies ε_ν correspond to $K = 20$ and $\delta = 2$. The gap between the most energetic eigenstate $|\Psi\rangle$ (red dot), preferentially populated at maximal driving and zero dephasing (see Eq. (S4)), and the conducting band, is of $\mathcal{O}(\delta)$.

The lattice is incoherently coupled to an auxiliary state $|s\rangle$ through its first ($|1\rangle$) and last ($|K\rangle$) states, with jump operators

$$\hat{V}_{\ell,r}^- = \sqrt{\Gamma(1 \mp f)} \hat{\Lambda}_{\ell,r}^-, \quad \hat{V}_{\ell,r}^+ = \sqrt{\Gamma(1 \pm f)} \hat{\Lambda}_{\ell,r}^+, \quad (\text{S2})$$

where $\hat{\Lambda}_\ell^- = |s\rangle\langle 1|$, $\hat{\Lambda}_r^+ = |K\rangle\langle s|$, $\hat{\Lambda}_\ell^+ = (\hat{\Lambda}_\ell^-)^\dagger$ and $\hat{\Lambda}_r^- = (\hat{\Lambda}_r^+)^\dagger$. In addition, the dephasing at rate γ corresponds to the jump operator (with identity \hat{I})

$$\hat{\Lambda}_z = \sqrt{\gamma}(\hat{I} - 2|K\rangle\langle K|), \quad (\text{S3})$$

which is equivalent to $\hat{\sigma}^z$ in the XXZ model and acts only on the state of highest energy. This is similar to the effect of dephasing on the original many-body system, which induces transitions from high-energy flat bands of the eigenstructure to low-energy wide bands of higher conduction [S2].

The NDC and the dephasing-assisted transport featured by this model are shown in Fig. S3(a) for $K = 10$, $\Gamma = 1$ and $\delta = 1$. Note that $\delta = 1$ does not correspond to the isotropic point of the XXZ model. The model does not capture the transport phase transition, as it is defined to mimic the strongly-interacting regime of the spin chain. Here δ sets the size of the gap between bands [S2]. We clearly see that when $\gamma = 0$ the system is insulating at maximal driving $f = 1$, where the equivalent of the ferromagnetic domains is a preferred population of state $|K\rangle$ (see Eq. (S4)). The NDC is washed out by dephasing, which results in a large transport enhancement with γ . For large dephasing the transport is degraded, as a result of the Zeno effect which tends to freeze the dynamics. Thus the main transport properties of the strongly-interacting XXZ system are captured by the minimal model.

The corresponding maximal values of the Leggett-Garg functions for operator \hat{Q} acting on the central site of the system are depicted in Fig. S3(b). At the insulating limit there is no LGI violation, but as the driving is diminished and/or dephasing increases, the violation emerges. Very large dephasing starts degrading this quantum behavior, as expected. The minimal model thus also captures the behavior of the quantumness measure.

S3. ANALYTIC RESULTS ON THE MINIMAL MODEL

In the following we describe an analytic approach to obtain the LGIs of the simple minimal model, focused on large driving and weak dephasing. We first note that in the maximally-driven limit $f = 1$ and in the absence of dephasing, this model features an insulating NESS akin to that of the original model of the main text, of the form [S2]

$$\hat{\rho}^{(0)} = \frac{1}{\mathcal{N}} |\Psi\rangle\langle\Psi|, \quad |\Psi\rangle = \sum_{n=0}^{K-1} (2\delta)^{-n} |K-n\rangle, \quad (\text{S4})$$

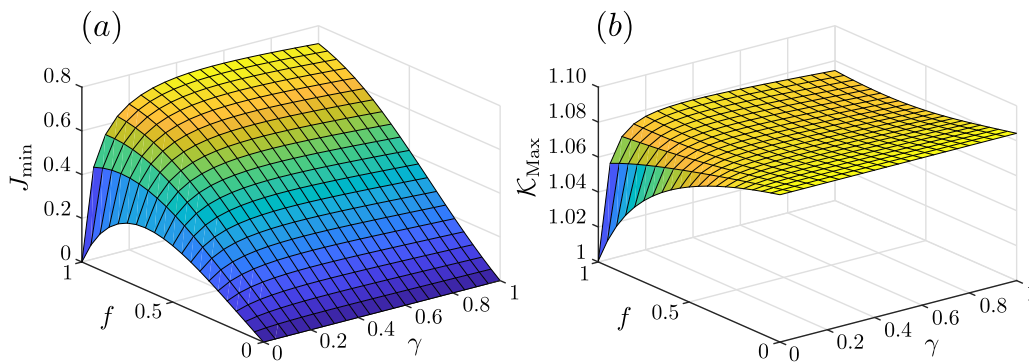


FIG. S3. **Physical properties of the minimal model.** (a) Current $J_{\min} = \langle \hat{J}_{\min,k} \rangle$ as a function of driving f and dephasing γ . (b) Corresponding maximal value of the Leggett-Garg function, i.e. maximal violation of LGI.

with normalization constant

$$\mathcal{N} = \frac{4\delta^2 - (4\delta^2)^{1-K}}{4\delta^2 - 1}. \quad (\text{S5})$$

This result shows that the population of a site exponentially decreases as it gets far from the rightmost site $|K\rangle$.

A. Perturbative $1 - f$ solution to the minimal model

Now we move from the maximally-driven case, and consider the situation where a weak back-flow is introduced, while keeping $\gamma = 0$. So we obtain the correction to the NESS to first order in $\mu = 1 - f \ll 1$, given by

$$\hat{\rho}_{\infty} = \hat{\rho}^{(0)} + \mu \hat{\rho}^{(1)}. \quad (\text{S6})$$

For this we rewrite the Lindblad superoperator of Eq. (2) of the main text in the form

$$\hat{\mathcal{L}}(\hat{\rho}) = \hat{\mathcal{L}}^{(0)}(\hat{\rho}) + \mu \hat{\mathcal{L}}^{(1)}(\hat{\rho}), \quad (\text{S7})$$

where $\hat{\mathcal{L}}^{(0)}(\hat{\rho})$ corresponds to the $\mu = 0$ Lindblad superoperator, namely

$$\hat{\mathcal{L}}^{(0)}(\hat{\rho}) = -i [\hat{\mathcal{H}}, \hat{\rho}] + \Gamma \left(\mathcal{D}_{\hat{\Lambda}_\ell^-} + \mathcal{D}_{\hat{\Lambda}_r^+} \right), \quad (\text{S8})$$

and $\hat{\mathcal{L}}^{(1)}(\hat{\rho})$ to the remaining terms,

$$\hat{\mathcal{L}}^{(1)}(\hat{\rho}) = \frac{\Gamma}{2} \left(\mathcal{D}_{\hat{\Lambda}_\ell^+} + \mathcal{D}_{\hat{\Lambda}_r^-} - \mathcal{D}_{\hat{\Lambda}_\ell^-} - \mathcal{D}_{\hat{\Lambda}_r^+} \right), \quad (\text{S9})$$

where each dissipator \mathcal{D} is given by

$$\mathcal{D}_{\hat{X}}(\hat{\rho}) = \hat{X} \hat{\rho} \hat{X}^\dagger - \frac{1}{2} \{ \hat{X}^\dagger \hat{X}, \hat{\rho} \}. \quad (\text{S10})$$

To solve Eq. (S7) for the NESS $\hat{\rho}_{\infty}$, we use the ansatz

$$\hat{\rho}_{\infty} = \sum_{p=0}^{\infty} \mu^p \hat{\rho}^{(p)}. \quad (\text{S11})$$

Gathering terms of equal powers of μ , we obtain the equations that determine the different order corrections. For $p = 0$, this corresponds to $\hat{\mathcal{L}}^{(0)}(\hat{\rho}^{(0)}) = 0$, which is the $\mu = 0$ equation with the solution of Eq. (S4). For $p > 0$ we have

$$\hat{\mathcal{L}}^{(0)}(\hat{\rho}^{(p)}) + \hat{\mathcal{L}}^{(1)}(\hat{\rho}^{(p-1)}) = 0, \quad (\text{S12})$$

The off-diagonal real values are

$$r_{0,1} = -\frac{1}{4\delta}, \quad r_{0,2} = -\frac{1}{2} \left(\frac{1}{2\delta} \right)^2. \quad (\text{S20})$$

The imaginary values correspond to the expectation value of the (homogeneous) NESS current, given by

$$j_1 = \langle \hat{J}_{\text{min},k} \rangle = \frac{1}{2} \Gamma \left(\frac{1}{2\delta} \right)^2. \quad (\text{S21})$$

Finally, the population of the auxiliary state is $r_s = 1/2$. We have verified numerically that these results indeed correspond to the correct solution to the linear system of equations, and thus give the correct form of the first-order correction $\hat{\rho}^{(1)}$.

B. LGIs violation enhancement by driving

Here we discuss the LG functions of the NESS of the strongly-driven minimal model. We first consider the $f = 1$ limit. Applying the operator $\hat{Q} = \hat{\mathcal{I}} - 2|P\rangle\langle P|$ to $\hat{\rho}^{(0)}$ we get

$$\hat{Q}\hat{\rho}^{(0)} = \hat{\rho}^{(0)} - \frac{2}{\mathcal{N}} \sum_{n=0}^{K-1} (2\delta)^{-(K-P+n)} |P\rangle\langle K-n|. \quad (\text{S22})$$

The dominant term of the sum is of $\mathcal{O}((2\delta)^{-(K-p)})$ (for $n = 0$), which is insignificant within the order $\mathcal{O}(\delta^{-2})$ of our solution if site P is far from the right boundary. Thus $\hat{Q}\hat{\rho}^{(0)} \approx \hat{\rho}^{(0)}$, and the time correlation is

$$\mathcal{C}^{(0)}(t) = \text{Tr} \left(\hat{Q} \exp[\hat{\mathcal{L}}^{(0)} t] \hat{Q} \hat{\rho}^{(0)} \right) \approx \text{Tr} \left(\hat{Q} \exp[\hat{\mathcal{L}}^{(0)} t] \hat{\rho}^{(0)} \right) = \text{Tr} \left(\hat{Q} \hat{\rho}^{(0)} \right) \approx \text{Tr}(\hat{\rho}^{(0)}) = 1. \quad (\text{S23})$$

It is approximately constant, as expected from the insulating nature of the state. The corresponding Leggett-Garg function is

$$\mathcal{K}^{(0)}(t) = 2\mathcal{C}^{(0)}(t) - \mathcal{C}^{(0)}(2t) \approx 1, \quad (\text{S24})$$

indicating that the LGI is not violated².

Now we consider the system slightly below maximal driving, namely with $\mu = 1 - f \ll 1$, whose NESS was discussed in Section . With the NESS of Eq. (S6) calculated up to first order in μ we can proceed to obtain the perturbative correction to the early-time time correlations $\mathcal{C}^{(1)}(t)$ and Leggett-Garg function $\mathcal{K}^{(1)}(t)$, so that

$$\mathcal{C}(t) = \mathcal{C}^{(0)}(t) + \mu \mathcal{C}^{(1)}(t), \quad (\text{S25})$$

$$\mathcal{K}(t) = \mathcal{K}^{(0)}(t) + \mu \mathcal{K}^{(1)}(t). \quad (\text{S26})$$

Expanding the time correlations in Eq. (3) of the main text up to second order in time, the perturbative correction to the $f = 1$ Leggett-Garg function is

$$\mathcal{K}^{(1)}(t) = -t^2 \text{Re} \left(\text{Tr} \left[\hat{Q} \hat{\mathcal{L}}^2 \hat{Q} \hat{\rho}^{(1)} \right] \right), \quad (\text{S27})$$

indicating that there is no linear correction in time for \mathcal{K} . To calculate it, first we note that applying \hat{Q} to $\hat{\rho}^{(1)}$ gives

$$\hat{Q}\hat{\rho}^{(1)} = \hat{\rho}^{(1)} - 2r_b |P\rangle\langle P| + 2ij_1 (|P\rangle\langle P+1| - |P\rangle\langle P-1|). \quad (\text{S28})$$

Applying the Lindblad operator $\hat{\mathcal{L}}$ twice to $\hat{Q}\hat{\rho}^{(1)}$ is a lengthy process, so we focused on obtaining the real diagonal terms which give a finite contribution to the trace after being multiplied again by \hat{Q} . We finally obtain

$$\text{Re} \left(\text{Tr} \left[\hat{Q} \hat{\mathcal{L}}^2 \hat{Q} \hat{\rho}^{(1)} \right] \right) = -2 \text{Re} \left(\text{Tr} |P\rangle\langle P| 2r_b |P\rangle\langle P| \right) = -4r_b, \quad (\text{S29})$$

² We have observed numerically that $\mathcal{K}^{(0)}(t)$ is actually slightly larger than one for short times, but since the governing term is

of $\mathcal{O}((2\delta)^{-(K-P)})$, such a violation is insignificant for $\delta > 1$.

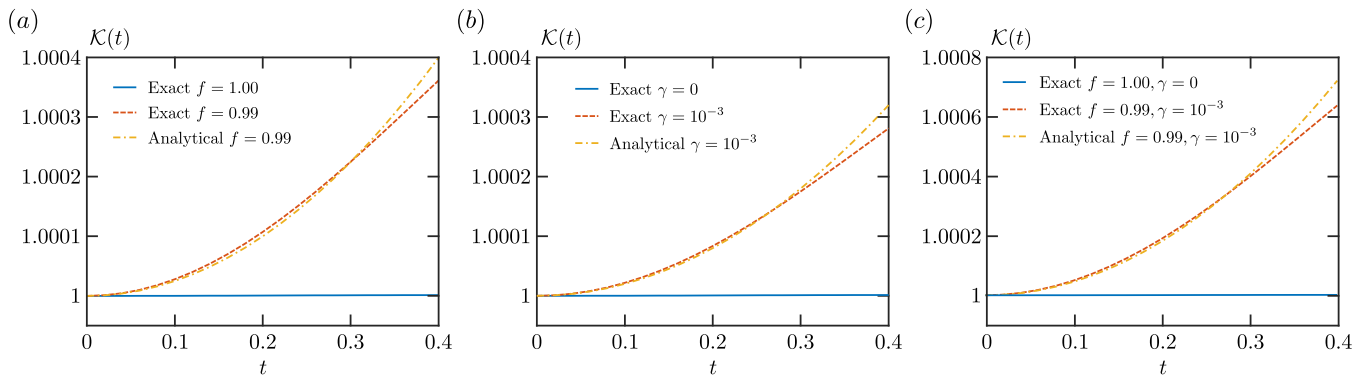


FIG. S4. **Comparison of analytical and numerical results for the minimal model.** The results correspond to $K = 10$, $\delta = 2$ and $\Gamma = 1$, (a) for $f = 0.99$ and $\gamma = 0$, (b) for $f = 1.00$ and $\gamma = 10^{-3}$, (c) for $f = 0.99$ and $\gamma = 10^{-3}$.

which, using Eq. (S19), gives that the correction of the LGI function is

$$\mathcal{K}(t) - \mathcal{K}^{(0)}(t) = 2(1-f)(1+\Gamma^2) \left(\frac{t}{2\delta} \right)^2. \quad (\text{S30})$$

Since this is a positive quantity and $\mathcal{K}^{(0)}(t) \approx 1$, we indeed observe that LGIs are violated when moving slightly away from the $f = 1$ scenario, and that such violation increases with time and as f decreases. In Fig. S4(a) we show that this prediction agrees well with exact numerical results for early times.

C. LGIs violation enhancement by dephasing

An identical calculation can be performed for the maximally-driven $f = 1$ limit, but with a weak dephasing rate $\gamma \ll 1$. However this can also be obtained considering the driving-dephasing equivalence in the minimal model described in Ref. [S2], both were seen to induce the same effect on the NESS when replacing

$$\gamma = \frac{1}{2}(1-f)\frac{\Gamma}{4}. \quad (\text{S31})$$

The correction to the Leggett-Garg function is then

$$\mathcal{K}(t) - \mathcal{K}^{(0)}(t) = 16\gamma \frac{(1+\Gamma^2)}{\Gamma} \left(\frac{t}{2\delta} \right)^2, \quad (\text{S32})$$

which is also positive and thus indicates that dephasing induces a violation of the LGIs, which increases with γ . This result is also in agreement with exact numerical calculations, as depicted in In Fig. S4(b). If both a weak backflow and dephasing are present, where both mechanisms enhance the LGI violations, the result is simply the sum of the independent contributions of Eqs. (S30) and (S32), namely

$$\mathcal{K}(t) - \mathcal{K}^{(0)}(t) = 2(1+\Gamma^2) \left[(1-f) + \frac{8\gamma}{\Gamma} \right] \left(\frac{t}{2\delta} \right)^2. \quad (\text{S33})$$

This additive enhancement of the two mechanisms is verified by exact numerical simulations, which as shown in Fig. S4(c), present a very good agreement.

[S1] N. Lambert, C. Emary, Y.-N. Chen, and F. Nori, Phys. Rev. Lett. **105**, 176801 (2010).

[S2] J. J. Mendoza-Arenas, T. Grujic, D. Jaksch, and S. R. Clark, Phys. Rev. B **87**, 235130 (2013).